The Egyptian Int. J. of Eng. Sci. and Technology
Vol. 17, No. 1 (Jan. 2014)

EIJES

EFFICIENCY OF VERTICAL SUSPENDED BREAKWATER SUPPORTED ON PILES*

El-sadek M. Heikal, Ayman S. Koraim, Ibrahim A. Elbagory.
Water Eng. Dept, Faculty of Engineering, Zagazig University, Egypt.

ABSTRACT:

The hydrodynamic efficiency of a proposed type of breakwaters was studied using numerical and physical models. The breakwater consists of caisson supported on a pile system and thin plates suspended on the piles under the caisson. A Flow-3D software which is based on the finite differences and volumes was used to examine the hydrodynamic efficiency of the suggested breakwater system. The efficiency of the breakwater was presented as a function of wave transmission, reflection and energy dissipation coefficients. Regular waves with different wave heights and periods and constant water depth were investigated. In addition, different characteristics of the caisson structure, the plates and the pile system were tested. It was found that the transmission coefficient (k_t) decreases with the relative caisson draft (D_1/h), the relative plate depths (D_2/h and D_3/h), the relative breakwater width (B/h), and the distance between piles (S) and piles diameters (d) and with decreasing the pile gap-diameter ratio (G/d).Also the reflection coefficient(k_r) and the energy dissipation coefficient (k_L) increases with the relative caisson draft (D_1/h), the relative plate depths (D_2/h and D_3/h), the relative breakwater width (B/h), the distance between piles (S) and the pile diameter (d) and with decrease of the pile gap-diameter ratio (G/d). The study shows that we can get (k_t) values less than 0.25 when $D_1/h \geq 0.5$, and also when $D_2/h, D_3/h \geq 0.4$at $D_1/h=0.1$. The reflection coefficient (k_r) values were between 15 to 55 % for all studied models. The proposed breakwater dissipates about 10 to 30 % of the incident wave energy. In addition, the study shows that the proposed breakwater model has about 75 % efficiency compared with other suspended floating breakwaters.

KEY WORDS: Breakwater; Caisson; Piles breakwater; Wave Transmission; Wave Reflection; Energy Loss.

EFFICACITÉ DU BRISE-LAMES VERTICAL SUSPENDU SUR PIEUX

RÉSUMÉ

L'efficacité hydrodynamique d'un type brise-lames a été étudiée à l'aide de modèles numériques et physiques. Le brise-lames se compose d'un caisson appuyé sur le système de apile et plaques minces en suspension sur les pieux sous le caisson. Un logiciel Flow- 3D qui s'appuie sur les différences et les volumes finis a été utilisée pour examiner l'efficacité hydrodynamique du système de brise-lames proposé. L'efficacité de la digue a été présentée comme une fonction de transmission d'onde, les coefficients de réflexion et de dissipation d'énergie. Vagues régulières avec différentes hauteurs et périodes vagues et la profondeur de l'eau constante ont été étudiés. En outre, les différentes caractéristiques de la structure de caisson, les plaques et le système de pile sont testés. On a constaté que le coefficient de transmission (kt) diminue avec l' ébauche par rapport à caisson (D1 / h) , la profondeur de la plaque relatifs (D2 / h et D3 / h), la largeur de la digue rapport (B / h) , et la distance entre les piles (S) et des diamètres de pieux (d) et avec la diminution du rapport écart - diamètre pile (G / d) . Aussi le coefficient de réflexion (kr) et le coefficient de dissipation d'énergie (kL) augmente avec le projet de caisson rapport (D1 / h) , la profondeur de la plaque par rapport (D2 / h et D3 / h), la largeur de la digue rapport (B / h), la distance entre les piles (S) et le diamètre du pieu (d) et avec diminution du rapport de poil écart de diamètre (G / D) . L'étude montre que nous pouvons obtenir (kt) des valeurs inférieures à 0,25 quand D1 / h ≥ 0,5 , et aussi quand D2 / h , D3 / h ≥ 0.4at D1 / h = 0,1 . Le coefficient de réflexion (kr) des valeurs comprises entre 15 à 55% pour tous les modèles étudiés . Le brise-lames dissipe environ 10 à 30 % de l'énergie de l'onde incidente. En outre, l'étude montre que le modèle de brise-lames a environ 75 % d'efficacité par rapport aux autres brise-lames flottants suspendus.

MOTS CLÉS: Brise-Lames; Caisson; Piles Brise-Lames; Transmission Onde; Réflexion Onde; Perte D'énergie.

* Received:10/6/2013, Accepted:19/1/2014, Ref. No. 154, (Original paper)
+ Contact author (ibrahimelbagory@yahoo.com)

1. INTRODUCTION:

Coastal environment, particularly beaches, are among the most dynamic of geomorphic environments. One of the phenomena's that beaches can be exposed to is shore erosion. Therefore shore protection against erosion play important role for increasing the national income by providing many of safe coastal regions and beaches which can be used in recreational and commercial activities such as harbors. The water waves have a great impact on shore line shore changes.

A relatively new type of vertical suspended breakwaters , Figure (1), will be studied to show its effect on waves, though alternative types such as Rubble mound and vertical submerged breakwaters was used before.

Vertical Suspended breakwaters are used to protect harbors and beaches from wave action and erosion by reducing the amount of water wave energy in their lee, and to initiate sediment deposition at the shoreline through the modification of near shore currents This type also offer an alternative to conventional fixed breakwaters, and it is inexpensive in construction and in maintenance (Koraim [7], 2005).

The functional performance of the caisson breakwater is evaluated by examining the wave reflection, transmission and energy dissipated due to the breakwater. Many experimental studies are presented for determining efficiency of this type as a function of transmission coefficient. Heikal [5], (2004) developed theoretical models using the Eigen function Expansion Method to determine the efficiency of the thin vertical breakwaters.

the efficiency of models similar to the proposed model. These models are mainly semi-immersed smooth solid walls, pontoons or bodies supported on one or more rows of widely or closely spaced piles.

The efficiency of the semi-immersed wall used as a breakwater was experimentally and theoretically studied, Ursell [19], (1947) Weigel [20], (1960) Reddy [15] and Neelamani [12], (1992) developed a theoretical solution for the partial transmission and reflection of gravity waves in deep waters. Lui and Abbaspour (1982) used the Boundary Integral Equation method for analyzing the interaction between the water wave and the semi-immersed thin vertical barriers. Losada et al.[9], (1992), Abul-Azm1, (1993), Heikal [5], (2004), and Koraim[7], (2005) carried out experimental studies covering wide ranges of waves and structure parameters to determine the

Many experimental and theoretical studies were carried out for determining the hydrodynamic performance of pontoon structures of different shapes or structures supported on piles. Kato et al.6, (1966), Brebner [2], and Ofuya (1968), Yamamoto [21],(1981), Carver [3], and Davidson (1983), Mani (1991), Murali [11], and Mani [10], (1997), and Tolba [18], (1998) investigated different types of pontoon structures used as breakwaters. Mani (1991), and Murali and Mani (1997) investigated experimentally the trapezoidal floating bodies connected with vertical closely spaced pipes at its bottom. The breakwater was tested under wave and wave-current environment. Neelamani [12], and Rajendran (2002) and Neelamani [13], and Vedagiri (2002) studied experimentally the hydrodynamic performance of the T-type breakwater and partially immersed twin vertical barriers connected by horizontal deck. The breakwater was tested under regular and random waves. Sundar and Subbarao (2002) and (2003) carried out experimental studies on the quadrant front face pile supported breakwaters. Heikal (2004), and Koraim (2005) investigated experimentally the efficiency of a partially immersed caisson structure supported on piles on both horizontal and sloped beaches. The breakwater efficiency was determined as a function of transmission coefficient only. Rageh and Koraim (2008) investigated experimentally and theoretically the efficiency of the caisson breakwater when the spacing between the supporting piles is large, for such case the effect of the pile in reflecting the waves is neglected. The breakwater efficiency was determined as a function of transmission, reflection, and energy loss coefficients.

In this study the efficiency of caissons supported on two or three rows of piles is experimentally and mathematically studied. The breakwater efficiency is measured as a function of transmission, reflection, and wave energy dissipation coefficients. The effect of different wave and structural parameters on the breakwater efficiency such as; wave length, wave period, breakwater draft, breakwater width, piles diameter, and spacing between piles are presented.

2. METHODOLOGY

2.1. Numerical Model

Flow-3d software is used to examine the hydraulic performance of the models of the suggested breakwaters system. The fundamental laws of mass, momentum and energy conservation were adopted in which the finite difference method was applied to solve these equations. The numerical algorithm used was called SOLA-VOF (Solution Algorithm-Volume of Fluid) (Flow Science Inc., 1997). The flow regions are subdivided into a grid of variable-sized rectangular cells. For each cell, values are retained for the basic flow quantities (e.g., velocity, pressure and density). The breakwater system in the software was placed in the grids with Fractional Area Volume Obstacle Representation (FAVOR) method. By doing so, geometry and grid of structures can be treated independently by this method as in figure (2)

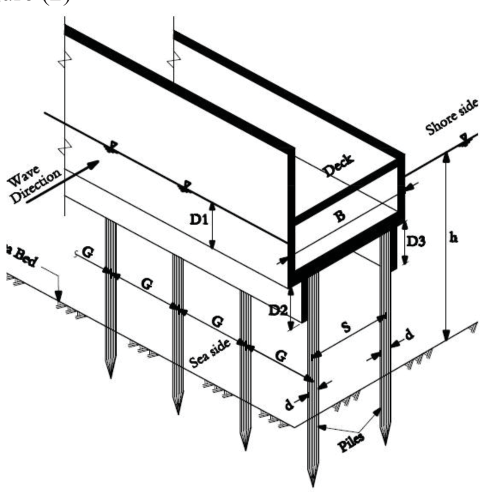

Fig. (1) Schematic diagram of 3D view of the Vertical Suspended Breakwater.

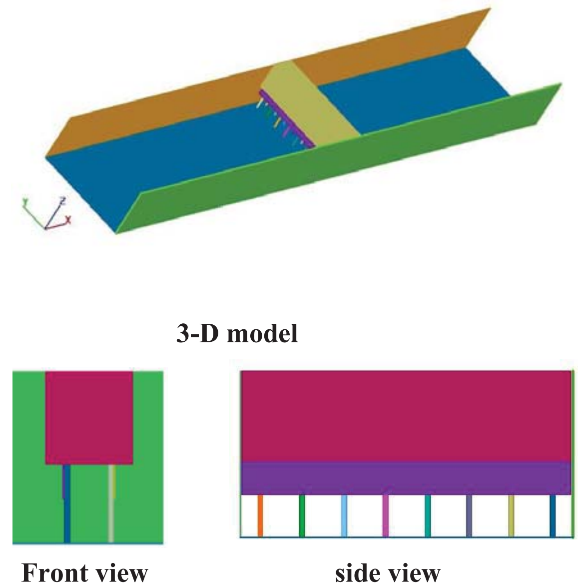

Fig. (2): Schematic diagrams of 3D view, Front and side views of flow-3d mathematical model.

2.2. Physical Model

The series of experiments are carried out for 9 different Suspended vertical floating breakwater supported on circular piles models in the wave flume 12.0 m long, 1.2 m deep, and 2 m wide in the Hydraulics and Water Engineering Laboratory of the Faculty of Engineering, Zagazig University, Zagazig, Egypt. Its vertical sides are made from reinforced concrete of 0.25 m thickness. A flap type wave generator with stroke distance of 0.3 m was installed at one end of the flume to generate regular wave trains with different wave periods. A gravel wave absorber with slope 3:1 was installed at the other end of the flume to absorb the transmitted waves. All experiments were carried out at a constant water depths of h = 0.5 m, Figure(3)

Fig. (3) Images of physical model, wave flume and wave generator.

2.3. Model Scale

According to Froude scaling a scale of 1:10 is chosen for the selection of model dimensions and wave properties in the present study. The proposed breakwater can be used for water depths ranging from 5 m to 10 m. However, the present study is carried out for a constant water depth of 0. 50 m, this corresponds to about 5 m water depth in the prototype.

2.4. Model Details

The tested breakwater model was placed at the middle of the wave flume and it was consisted of two parts. The upper part consists of a fixed box with width B and draft D_1 and two plats of depths D_2, D_3 respectively located under the fixed box in upstream and down stream and supported on the lower part which consists of two or three rows of piles with diameter d, center to center gap between piles G, and distance between the centerlines of the piles rows S. The details of the tested breakwater models are shown in Figures (1),(4).

2.5. Wave Gauge

The wave heights were measured using a movable Non-Contact Ultrasonic Distance Transmitter (NCUDT). This instrument consists of two main parts: (1) sensor part; and (2) digital screen.

The instrument measures the distance between the sensor part and the water surface ultrasonically with an accuracy of 1.0%. The reading appears digitally on a screen. The NCUDT unit was connected with a computer system for storing the output data. Then the variation of water surface with time can be drawn. It should be noted that the NCUDT unit is placed over a small carriage moving along the test channel length.

2.6. Incident, Reflected, and Transmitted Wave Heights

To measure the incident (H_i) and reflected (H_r) wave heights, two recording positions (P2 and P1) were set in front of the breakwater model (wave generator side) at distances 0.2L and 0.7L respectively where L is wave length. This is according to the two-point method of Goda and Suzuki 4, (1976). To measure the transmitted (H_t) wave heights, one additional recording position (P3) was set behind the breakwater model (wave absorber side) at a distance 2.0 m form the breakwater side of the shore. Details of wave flume, position of the tested breakwater model, and locations of wave recording are shown in Figure 4.

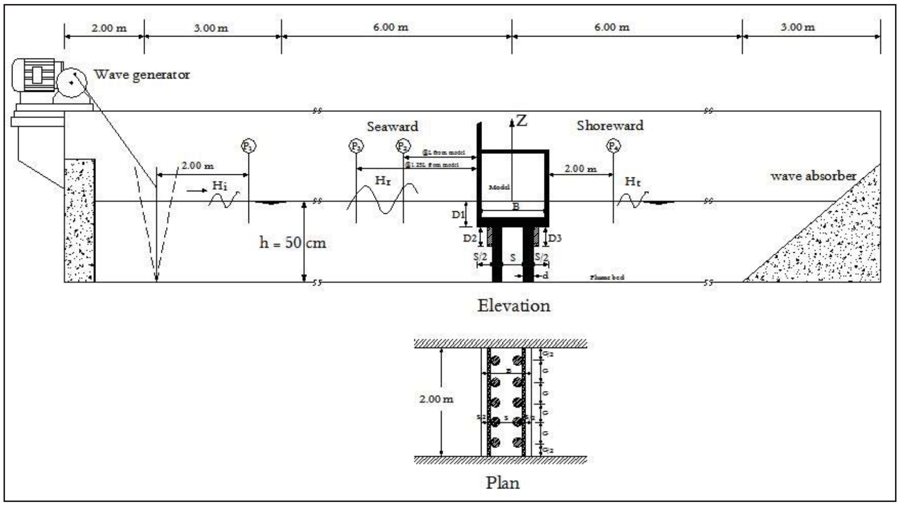

Fig. (4) Definition sketch for the breakwater model in the wave flume.

2.7. Reflection, Transmission, and Energy Dissipation Coefficients

The reflection (k_r) and the transmission (k_r) coefficients can be estimated from the experimental data as follows

$k_r = H_r / H_i$ (1)

$k_t = H_t / H_i$ (2)

Actually, when the wave reaches the structure, part of the incident wave energy is dissipated. This dissipated part of the wave energy can be estimated as a function of the reflection and transmission coefficients as given by Reddy and Neelamanit 1992: $k_L = 1 - k_r^2 - k_t^2$ (3) .

In which k_L is the wave energy dissipation coefficient.

3. NUMERICAL MODEL SETUP AND CALIBRATION

Flow-3D was used for determination the efficiency of the purposed model. The procedure followed to set up the numerical model and to carry out the simulation is shown in Figure (5). The governing equations are presented in as follows

These partial differential equations are converted to simple algebraic equations by some approximations. In relation with the discretization of the equations .the problem domain is also divided into discrete components which will be referred as the computational mesh.

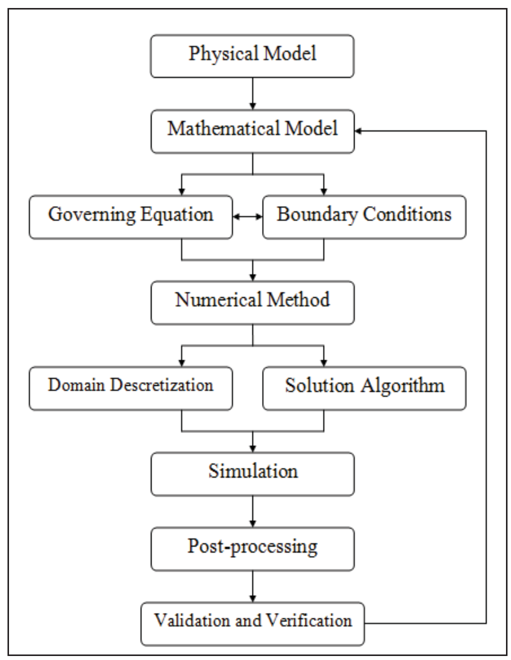

Fig. (5) Procedure for numerical simulations (Versteeg and Malalasekera, 1995).

For a fluid continuum governing equations are derived from the conservation laws for mass, momentum and energy. The mass conservation equation is:

$\partial\rho / \partial t + \Delta.(\rho v) = S_s$ (4)

Where (ρ) is the mass density of the fluid, (v) is the velocity vector and (Δ) is the gradient operator. (S_s) on the right hand side the equation represents the sources and sinks. In the absence of mass sources and incompressible flows the mass conservation equation reduces to the divergence of the velocity which is written as:

$\Delta.v = 0$ (5)

The momentum transport equation for the average flow field is:

$\rho\ (\partial v / \partial t + v.\ \Delta v) = -\ \Delta\ p - \Delta.\tau + Б$. (6)

Here, (Б) is the body force vector, (τ) is the viscous stress tensor and (p is the pressure. The momentum transport equation for the fluid continuum reduces to the Na+vier-Stokes equations for Newtonain fluids for which stress is linearly proportional to strain. For an incompressible fluid with constant viscosity, the Navier-Stokes equations can be written as:

$\rho\ (\partial v / \partial t + v.\ \Delta v) = -\ \Delta\ p - \mu\Delta^2 v + Б$ (7)

Where (μ) is the dynamic viscosity. Flow-3D solves these equations using finite difference and finite volume approximations. The domain was divided to 3 parts. The first and the third parts which located at up stream and down stream the model divided into large number of meshes. The second part is at the model site divided to number of meshes more than the first and the third part to more accuracy as shown in figure (6).

4. ANALYSIS AND RESULTS:

About 300 of experimental and numerical runs were carried to evaluate the hydrodynamic efficiency of the purposed model. Two parameters studied, a- waves parameters are wave length and period (L, T). b-The structural parameters are the caisson draft, sheets heights and width

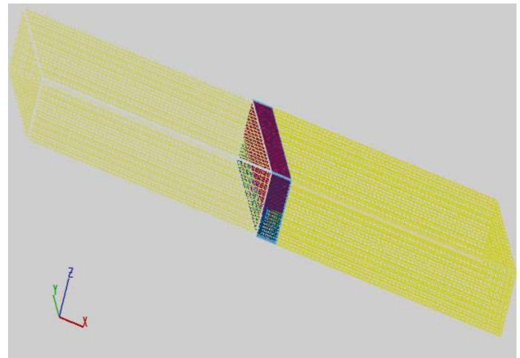

Fig.(6) Arrangement of multi-block mesh in computational domain of FLOW-3D

(D_1,D_2,D_3, B) and supporting pile system characteristics are pile diameter, gap between piles, and distance between rows of piles (d, G, S). The analysis presents the efficiency of the breakwater in the form of relationships between transmission, reflection, and energy dissipation coefficients (k_t, k_r, k_L) and dimensionless parameters representing the wave and structure characteristics as in the following equation:

$k_t,\ k_r,\ k_L = f\ (D_1/h,\ D_2/h,\ D_3/h, B/h, G/d, S/d, d/h\ )$ (8)

Figure (7) presents the comparison between the measured and the calculated hydrodynamic coefficients. Although the over all agreement is acceptable, the figure shows somewhat over-predict the transmission and the reflection coefficients at smaller values, while under-predicting them at larger values. Also, a good agreement is obtained between the estimated and the experimental data of the wave energy dissipation.

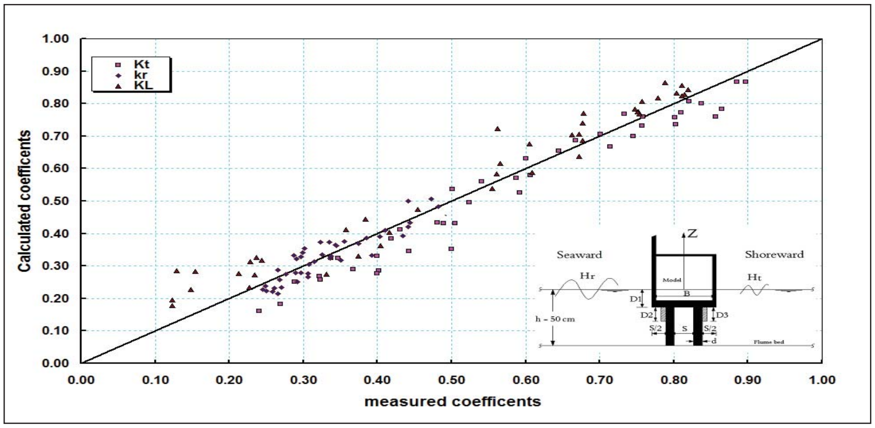

Fig.(7) Verification of numerical model FLOW 3-D results using experimental results.

Figure (8) show the comparison between Experimental and numerical results for different hydrodynamic coefficients k_t, k_r, k_L and the relative water depth h/L when D_1= 0.1h,D_2= D_3=0.4h, d=0.1h,S=0.5h,G=0.4h and B=h.The figure shows that, the values of the hydrodynamic coefficients k_t, k_r, k_L calculated from numerical models are very near from the values of the experimental models, the figure shows that the differences between numerical and experimental results is about less than 10 % and that is acceptable.

Figure (9) presents the relationship between k_t, k_r, k_L and h/L for different D_1/h values when d=0.1h, S=0.5h, G=0.4h, D_2=D_3=0 and B=h.
The figure shows that, k_t decreases with increasing of h/L and D_1/h. In which, k_t decreases from about 0.90 to 0.35, 0.90 to 0.25, 0.80 to 0.25 , 0.75 to 0.2 and 0.71 to 0.12 for D_1/h =0.1, 0.2, 0.3,0.4 and 0.5 respectively. The reflection coefficient (k_r) takes an opposite trend of k_t, in which, k_r ranges from about 0.33 to 0.65, 0.37 to 0.70, 0.41 to 0.77 , 0.50 to 0.90 and 0.53 to 0.95 for D_1/h =0.1, 0.2, 0.3,0.4 and 0.5 respectively. The energy dissipation coefficient (k_L) slightly increasing with increasing of D_1/h and h/L. In which, k_L ranges from about 0.43 to 0.72, 0.47 to 0.73, 0.37 to 0.65 , 0.45 to 0.48 and 0.5 to 0.42 for D_1/h =0.1, 0.2, 0.3,0.4 and 0.5 respectively.

Figure (10) presents the relationship between k_t, k_r, k_L and h/L for different D_2/h values when d=0.1h, S=0.5h, G=0.4h, D_1=0.1h, D_3=0 and B=h.
The figure shows that, k_t decreases with increasing of h/L and D_2/h. In which, k_t decreases from about 0.95 to 0.36, 0.90 to 0.35, 0.88 to 0.30 and 0.80 to 0.28 for D_2/h =0.1, 0.2, 0.3 and 0.4 respectively. The reflection coefficient (k_r) takes an opposite trend of k_t, in which, k_r ranges from about 0.38 to 0.74, 0.40 to 0.77, 0.45 to 0.87 and 0.52 to 0.91 for D_2/h =0.1, 0.2, 0.3 and 0.4 respectively. The energy dissipation coefficient (k_L) slightly increasing with increasing of D_2/h and h/L. In which, k_L ranges from about 0.18 to 0.65, 0.32 to 0.60, 0.30 to 0.47 , and 0.37 to 0.35 for D_2/h =0.1, 0.2, 0.3 and 0.4 respectively.

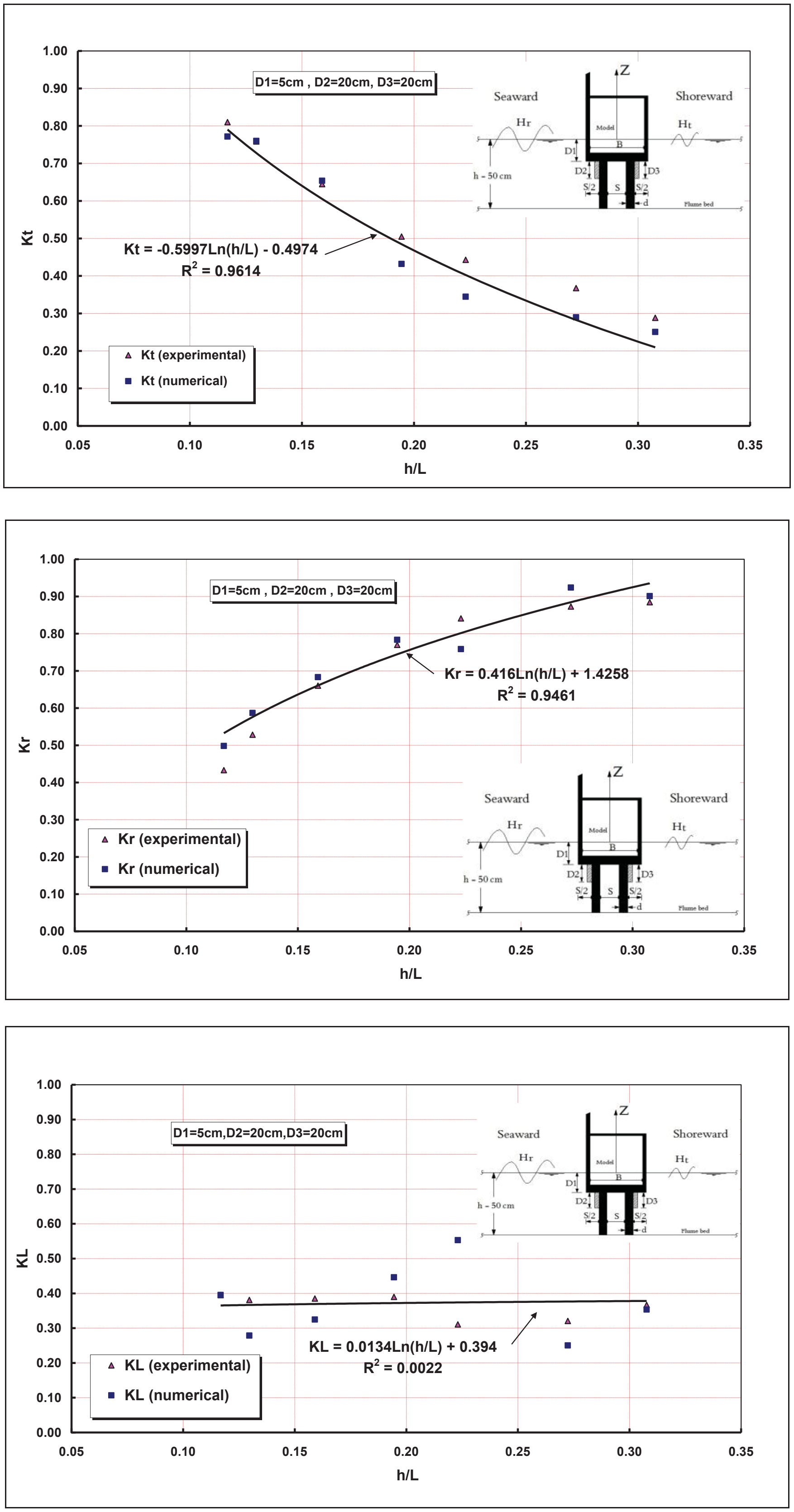

Fig. (8) Comparison between transmission, reflection and energy dissipation coefficients(d=0.1h, S=0.5h,G=0.4h ,D_1=0.1h and D_2=D_3=0.4h and B=h).

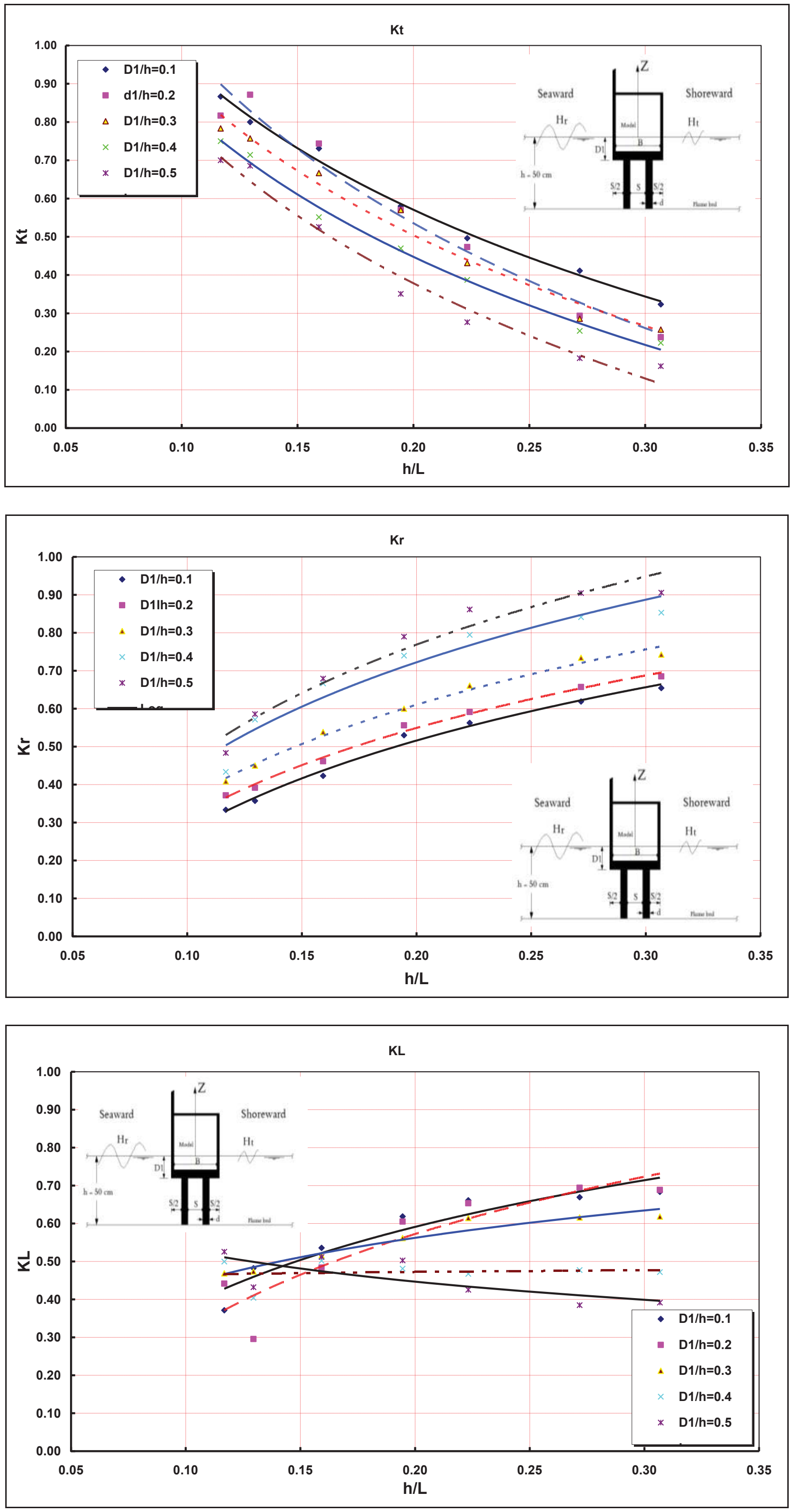

Fig. (9) Effect of D_1 on transmission, reflection and energy dissipation coefficients (d=0.1h, S=0.5h, G=0.4h, D_2=D_3=0 and B=h).

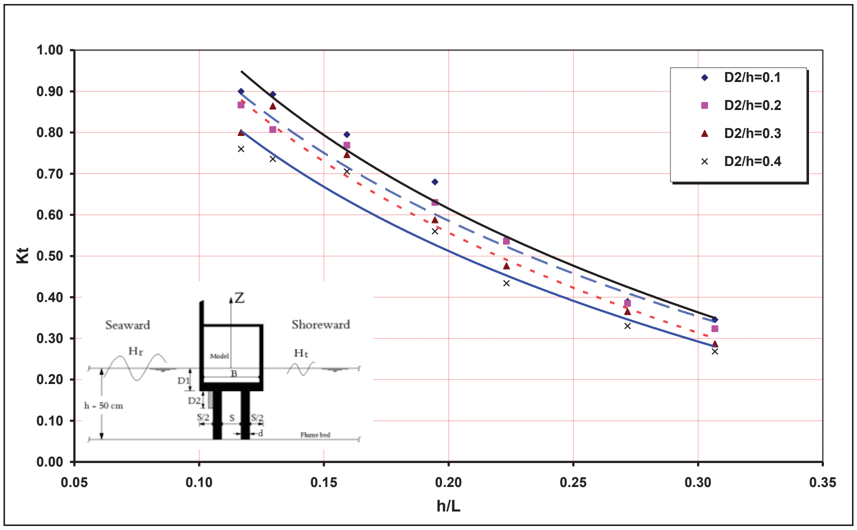

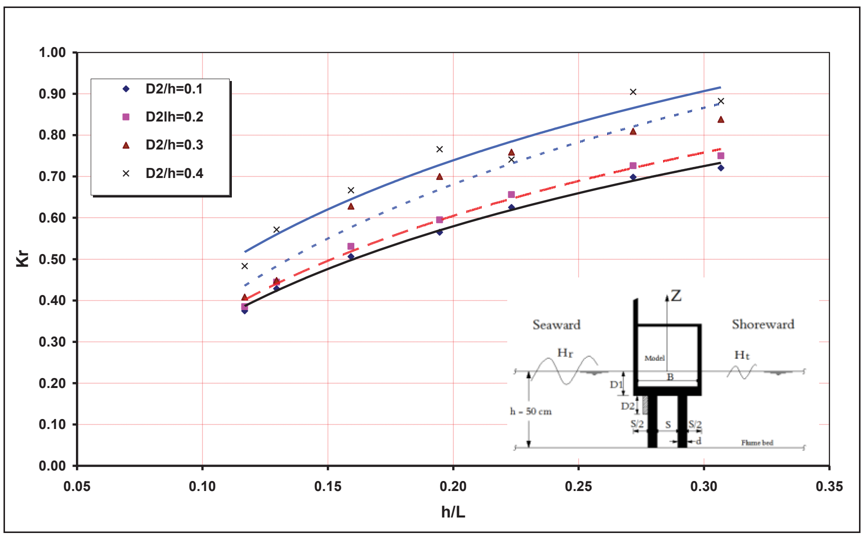

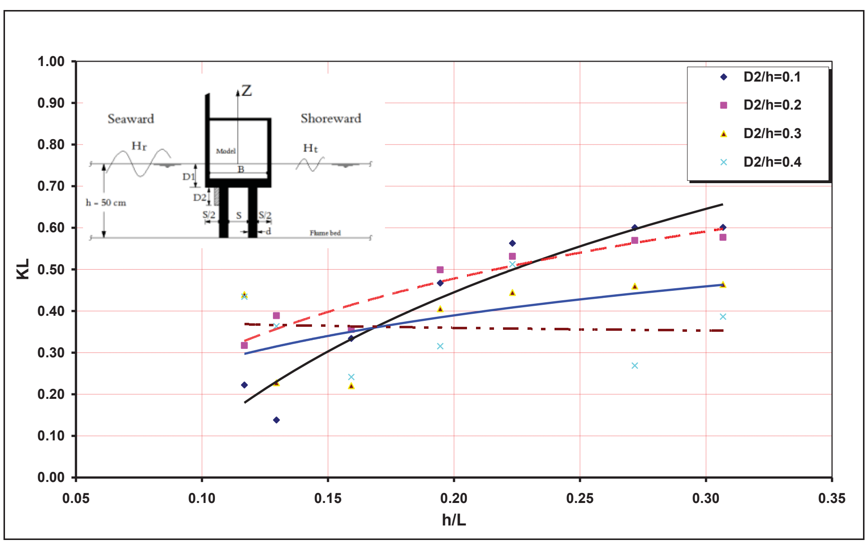

Fig. (10) Effect of D_2 on Transmission, reflection and energy dissipation coefficients (d=0.1h, S=0.5h, G=0.4h, D_1=0.1h, D_3=0 and B=h).

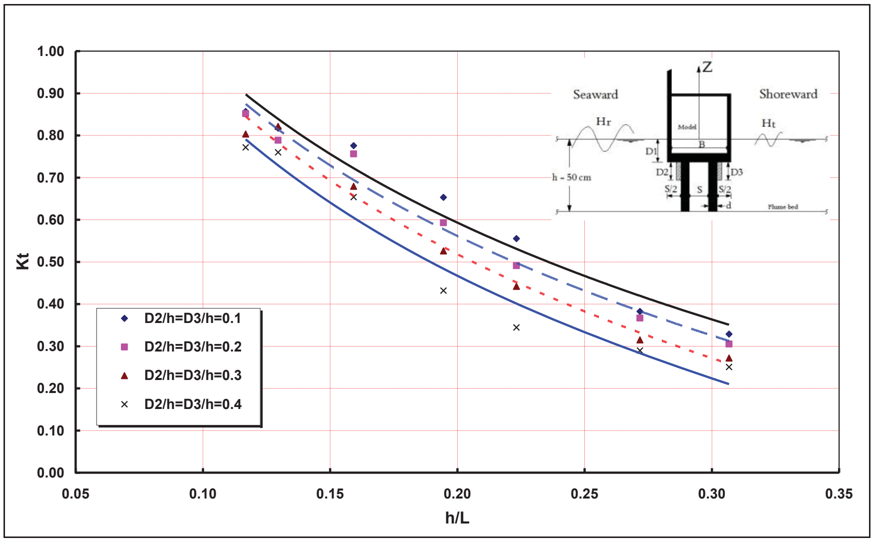

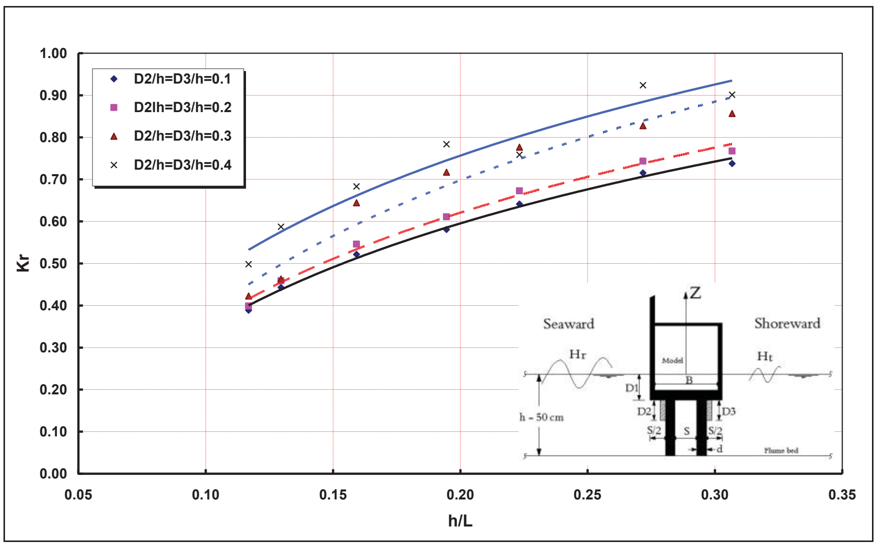

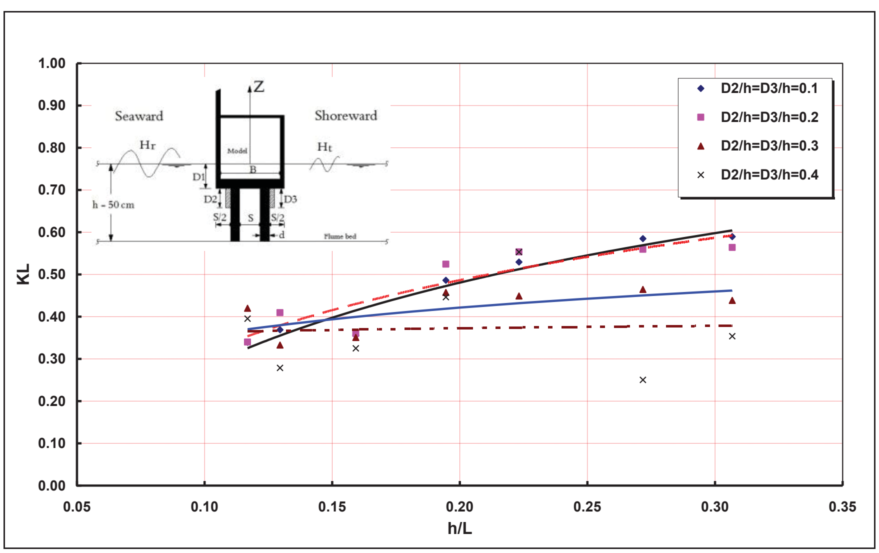

Fig.(11) Effect of D_2 and D_3 on Transmission, reflection and energy dissipation ($d=0.1h$, $S=0.5h$, $G=0.4h$, $D_1=0.1h$ and $B=h$).

Figure (11) presents the relationship between k_t, k_r, k_L and h/L for different D_2/h and D_3/h values when d=0.1h, S=0.5h, G=0.4h, D_1=0.1h and B=h.
The figure shows that, k_t decreases with increasing of h/L, D_2/h and D_3/h. In which, k_t decreases from about 0.90 to 0.35, 0.87 to 0.31, 0.85 to 0.27 and 0.80 to 0.21 for D_2/h= D_3/h =0.1, 0.2, 0.3 and 0.4 respectively. The reflection coefficient (k_r) takes an opposite trend of k_t, in which, k_r ranges from about 0.40 to 0.75, 0.42 to 0.78, 0.45 to 0.90 and 0.52 to 0.93 for D_2/h= D_3/h =0.1, 0.2, 0.3 and 0.4 respectively. The energy dissipation coefficient (k_L) slightly increasing with increasing of D_2/h, D_3/h and h/L. In which, k_L ranges from about 0.33 to 0.60, 0.36 to 0.58, 0.37 to 0.46 , and 0.36 to 0.38 for D_2/h= D_3/h =0.1, 0.2, 0.3 and 0.4 respectively.

Figure (12) presents the relationship between k_t, k_r, k_L and h/L for different B/h values when d=0.1h, S=0.5h, G=0.4h, D_1=0.1h and D_3= D_3 =0.4h.
The figure shows that, k_t decreases with increasing of h/L and B/h. In which, k_t decreases from about 0.85 to 0.25, 0.81 to 0.21, 0.77 to 0.20 and 0.74 to 0.18 for B/h =0.5, 1,1.5 and 2 respectively. The reflection coefficient (k_r) takes an opposite trend of k_t, in which, k_r ranges from about 0.48 to 0.91, 0.52 to 0.93, 0.56 to 0.95 and 0.64 to 0.98 for B/h=0.5, 1, 1.5 and 2 respectively. The energy dissipation coefficient (k_L) slightly increasing with increasing of B/h and h/L. In which, k_L ranges from about 0.28 to 0.45, 0.37 to 0.35, 0.38 to 0.39 , and 0.28 to 0.27 for B/h =0.5, 1, 1.5 and 2 respectively.

Figure (13) presents the relationship between k_t, k_r, k_L and h/L for different G/d values when d=0.1h, S=0.5h, B=h, D_1=0.1h and D_3= D_3 =0.4h.
The figure shows that, k_t decreases with increasing of h/L and decreases of G/d. In which, k_t decreases from about 0.74 to 0.17, 0.75 to 0.18, 0.78 to 0.20 and 0.80 to 0.21 for G/d =1, 2,3 and 4 respectively. The reflection coefficient (k_r) takes an opposite trend of k_t, in which, k_r ranges from about 0.64 to 0.98, 0.58 to 0.96, 0.56 to 0.94 and 0.52 to 0.93 for G/d =1, 2, 3 and 4 respectively. The energy dissipation coefficient (k_L) slightly increasing with increasing of h/L and decreasing of G/d. In which, k_L ranges from about 0.28 to 0.42, 0.35 to 0.30, 0.37 to 0.38, and 0.37 to 0.35 for G/d =1, 2, 3 and 4 respectively.

Figure (14) presents the relationship between k_t, k_r, k_L and h/L for different S/d values when d=0.1h, B=h, G=0.4h, D_1=0.1h and D_3= D_3 =0.4h.
The figure shows that, k_t decreases with increasing of h/L and S/d. In which, k_t decreases from about 0.84 to 0.25, 0.8 to 0.21, 0.76 to 0.20 and 0.75 to 0.19 for S/d =3, 5,7 and 9 respectively. The reflection coefficient (k_r) takes an opposite trend of k_t, in which, k_r ranges from about 0.50 to 0.90, 0.52 to 0.93, 0.56 to 0.95 and 0.59 to 0.98 for S/d =3, 5, 7 and 9 respectively. The energy dissipation coefficient (k_L) slightly increasing with increasing of S/d and h/L. In which, k_L ranges from about 0.32 to 0.45, 0.37 to 0.35, 0.38 to 0.34 , and 0.35 to 0.25 for S/d =3, 5, 7 and 9 respectively.

.

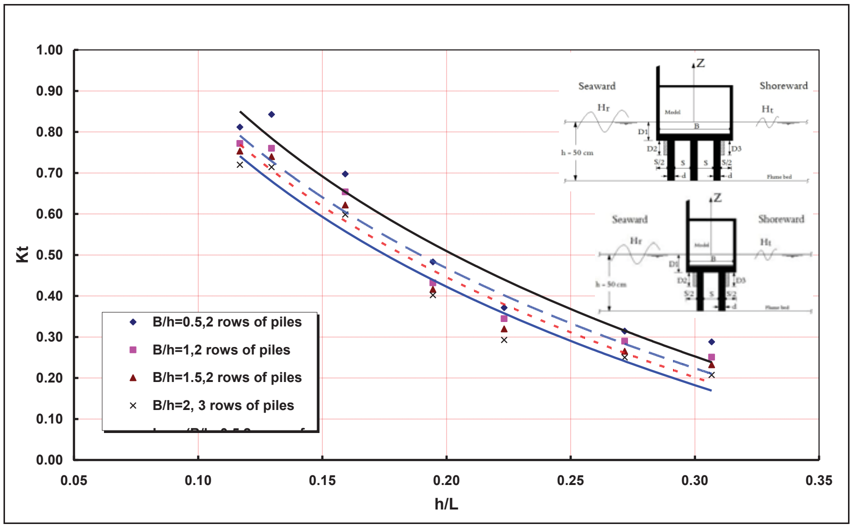

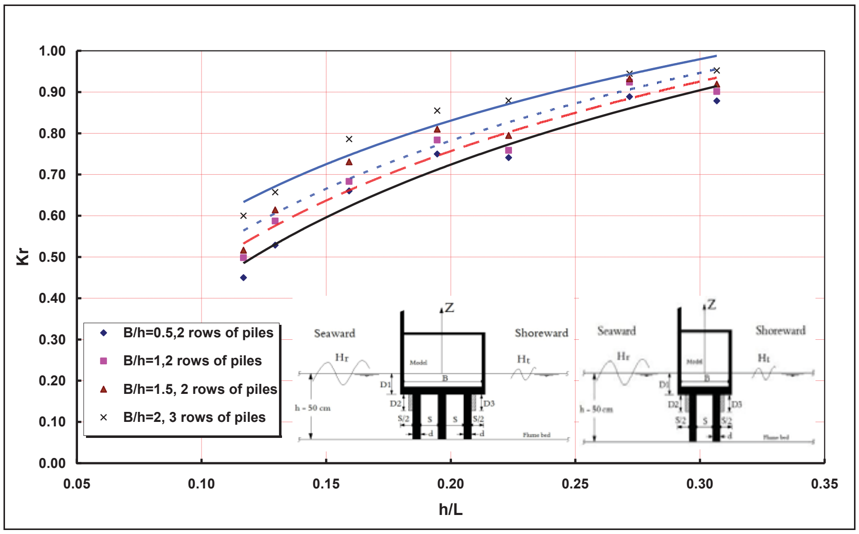

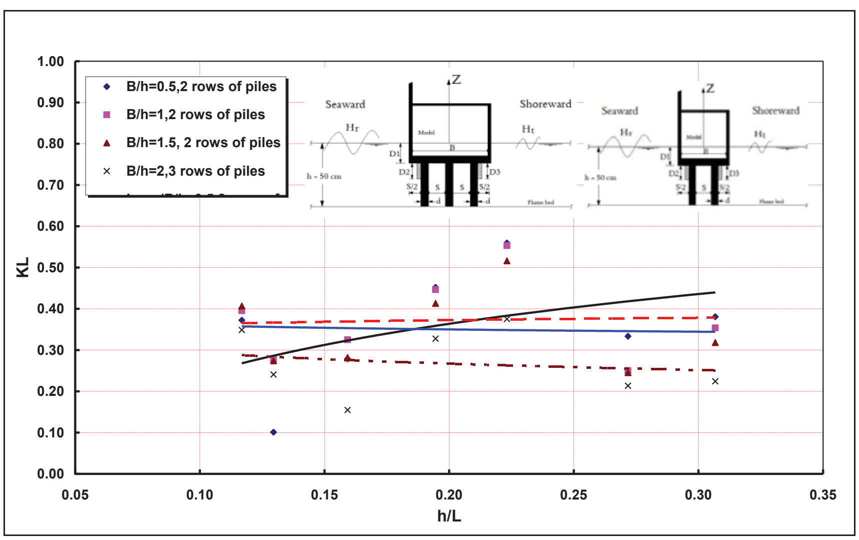

Fig.(12) Effect of B on transmission, reflection and energy dissipation coefficients (d=0.1h, S=0.5h, G=0.4h, D_1=0.1h and D_2=D_3=0.4h)

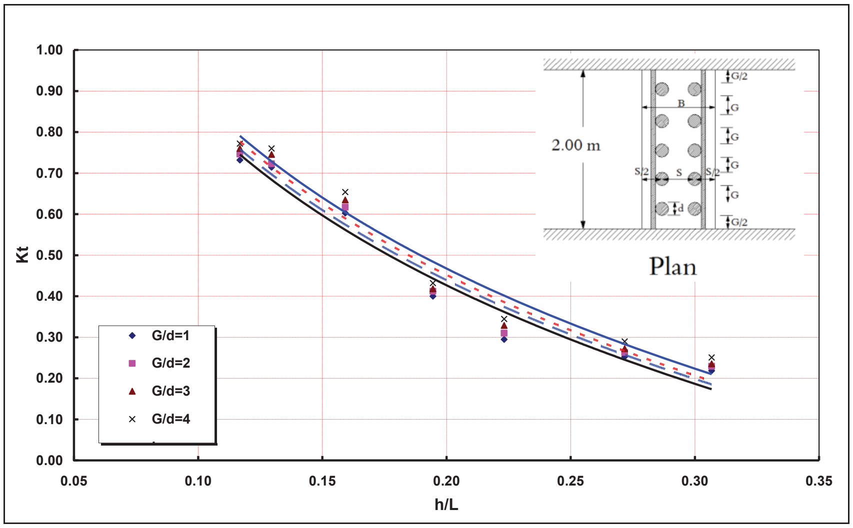

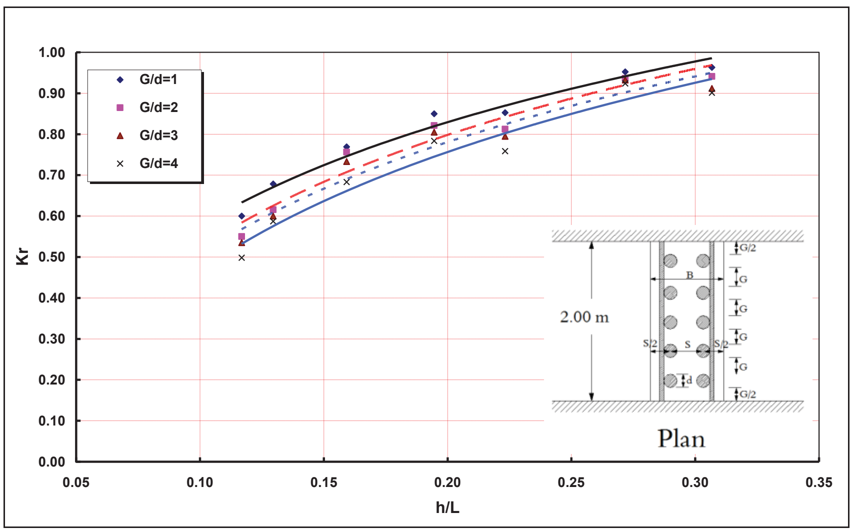

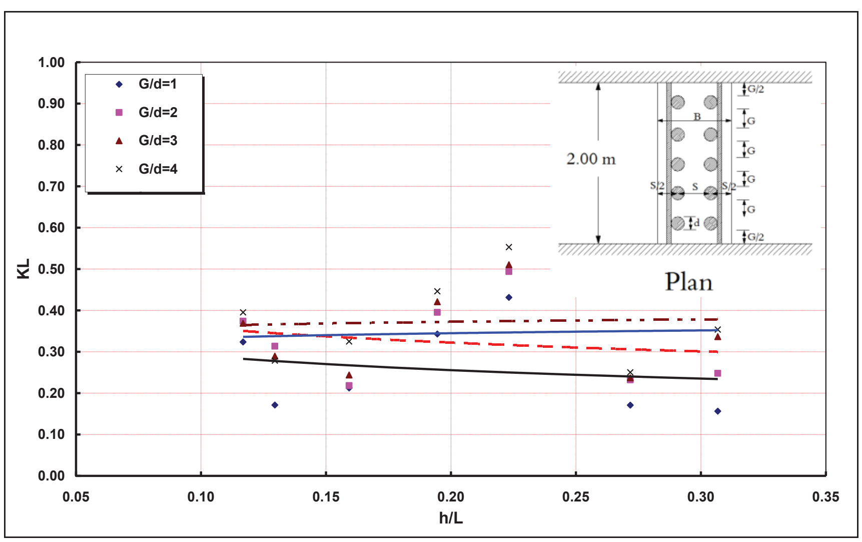

Fig.(13) Effect of G on transmission, reflection and energy dissipation coefficients ($d=0.1h$, $S=0.5h$, $B=h$, $D_1=0.1h$ and $D_2=D_3=0.4h$).

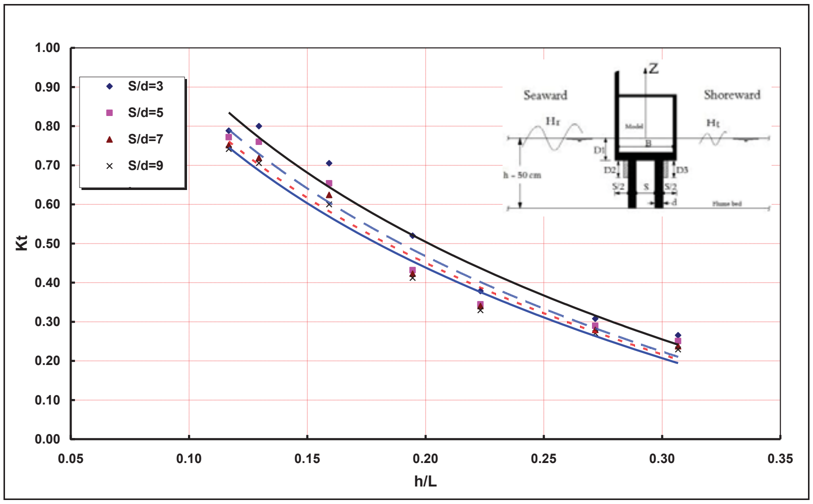

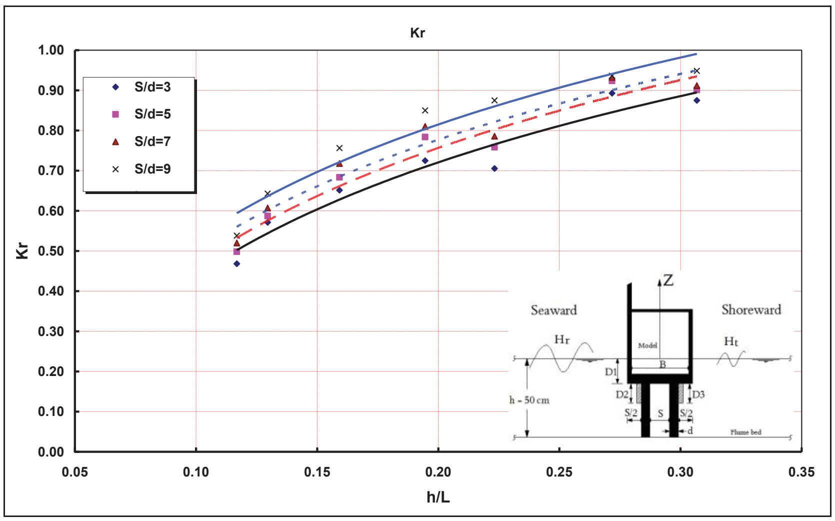

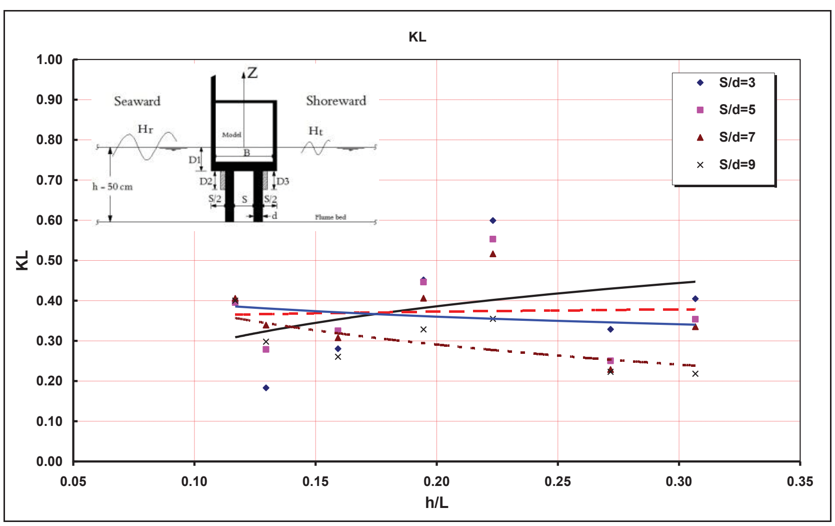

Fig. (14) Effect of S on transmission, reflection and energy dissipation coefficients (d=0.1h, G=0.4h, B=h, D_1=0.1h and D_2=D_3=0.4h).

5. CONCLUSIONS

The efficiency of proposed breakwater, which consists of caissons and sheets supported on two or three rows of piles, was studied using physical and mathematical models. The wave transmission, reflection, and energy dissipation characteristics were studied for regular waves. The analysis of the study of those models gives those results:

(i). The FlOW -3D theoretical model underestimate the transmission coefficient by about 5 - 10%.

kt theoretical = 1.06 measured - 0.0764 (fitted equation)

(ii). The proposed theoretical model underestimates the reflection coefficient by about 5 - 10%.

$K_{r\ theoretical} = 1.0566\ k_{r\ measured} - 0.0208$ (fitted equation)

(iii). The proposed breakwater helps in dissipating about 5 to 30 % from the incident wave energy. This wave dissipation increases as the breakwater width increases.

(iv). The efficiency of the proposed breakwater in reducing the transmitted waves becomes high as the breakwater width (B)equals or more the water depth when the relative breakwater drafts (D_1/h) equals or more than 0.5 and (D_2/h),(D_3/h) equals or more than 0.4

(v). The reflection coefficient increases as the relative breakwater width (B/h) increases when the relative breakwater drafts (D_1/h) equals or more than 0.5 and (D_2/h),(D_3/h) equals or more than 0.

Notations0

Symbol	Definition
B	Breakwater width;
d	Pile diameter;
D_1	Breakwater draft;
D_2	height of sheets supported on first row of piles;
D_3	height of sheets supported on last row of piles;
g	Acceleration of gravity;
G	Distance between piles center to center;
h	Water depth at the breakwater site;
H_i	Incident wave height;
H_r	Reflected wave height;
H_t	Transmitted wave height;
μ	Dynamic viscosity;
k_L	Energy dissipation coefficient;
k_r	Reflection coefficient;
k_t	Transmission coefficient;
L	Wave length at breakwater site;
S	Space between rows of piles center to center;
T	Wave period;
τ	Viscous stress tensor;
ρ	Water density;
v	Velocity vector;
P	Pressure;
Б	The body force vector;
S_s	Sources and sinks, and
Δ	= Gradient operator.

REFERENCES

1- Abul-Azm, A. G. Wave diffraction through submerged breakwaters, Journal of Waterway, Port, Coastal and Ocean Engineering 119 (6), 587-605, 1993.

2- Brebner, A., Ofuya, A. O. Floating breakwaters, In: Proceeding of fifth Coastal Engineering Conference, 1055-1085, 1968.

3- Carver, R. D. Davidson, D. D. Slopping floating breakwater model study, In: Proceeding of the Specialty Conference on Design Construction, Maintenance and Performance of Coastal Structures, 83A, 417-432 ,1983.

4- Goda, Y. Suzuki, Y., Estimation of incident and reflected waves in random wave experiments, In Proceeding of the 15th Coastal Engineering Conference, 828-845 ,1976..

5- Heikal, E. M Shore or marina protection using a closed frame fixed on piles. The Egyptian Journal for Engineering Sciences and Technology, Faculty of Engireeng, Zagazig University. 8 (1), 49-60, 2004.

6- Kato, J., Hagino, S., Uekita, Y . Damping effect of floating breakwaters, Journal of Waterways and Harbour Division 95 (3), 1068-1078, 1966.

7- Koraim, A. S. Suggested model for the protection of shores and marina. A Thesis of Ph. D. in Civil Engineering, Zagazig University, Zagazig, Egypt, 2005.

8- Liu, P. L.F., Abbaspour, M. Wave scattering by a rigid thin barrier. Journal of Waterway, Port, Coastal and Ocean Engineering 108 (4), 479-491, 1982 .

9- Losada, I. J., Losada, M. A., Roldan, A. J. Propagation of oblique incident waves past rigid vertical thin barrier. Applied Ocean Research 14, 191-199 , 1992.

10- Mani, J. S. Design of Y-frame floating breakwater. Journal of Waterway, Port, Coastal and Ocean Engineering 117 (2), 105-119, 1991.

11- Murali, K., Mani, J. S. Performance of cage floating breakwater. Journal of Waterway, Port, Coastal and Ocean Engineering 123 (4), 172-179., 1997.

12- Neelamani, S., Rajendran, R. Wave interaction with T-type breakwaters. Ocean Engineering 29, 151-175., 2002.

13- Neelamani, S., Vedagiri, M. Wave interaction with partially immersed twin vertical barriers. Ocean Engineering 29, 215-238, 2002.

14- Rageh, O. S., Koraim, A. S. Efficiency of partially immersed caissons as a breakwaters. In: Proceeding of sixth International Engineering Conference, Mansoura University, 2008

15- Reddy, M. S., Neelamanit, S. Wave transmission and reflection characteristics of a partially immersed rigid vertical barrier. Ocean Engineering 19, 313-325, 1992.

16- Sundar, V., Subbarao, B. V. V. Hydrodynamic pressures and forces on quadrant front face pile supported breakwater. Ocean Engineering 29, 193-214, 2002.

17- Sundar, V., Subbarao, B. V. V. Hydrodynamic performance characteristics of quadrant front-face pile-supported breakwater. Journal of Waterway, Port, Coastal and Ocean Engineering 129 (1), 22-33., 2003

18- Tolba, E. R. Behavior of floating breakwater under wave action, Ph. D. Thesis, Suez Canal University, Egypt., 1998.

19- Ursell, F. The effect of a fixed vertical barrier on surface waves in deep water. In: Proceeding of the Cambridge Philosophical Society 43 (3), 374-382., 1947.

20- Wiegel, R. L. Transmission of wave past a rigid vertical thin barrier. Journal of Waterways and Harbour Division 86 (1), 1-12, 1960.

21- Yamamoto, T. Moored floating breakwater response to regular and irregular waves, Applied Ocean Research 3, 114-123, 1981.

22- Flow Science Inc. Flow-3D Excellent in Flow Modeling Software, Flow-3D version 8.2. User Manual. Los Alamos. NM.97., (1997).